Magn Reson Med Sci 2023; 22; 117–125
doi:10.2463/mrms.tn.2021-0106
Published Online: December 11, 2021

TECHNICAL NOTE

Ultra-short Echo-time MR Angiography Combined with a Subtraction Method to Assess Intracranial Aneurysms Treated with a Flow-diverter Device

Yusuke Ayabe[1], Kohei Hamamoto[2,3*], Yoshikazu Yoshino[4,5], Yoshimasa Ikeda[1], Emiko Chiba[6], Hironao Yuzawa[3], and Noriko Oyama-Manabe[3]

A flow-diverter (FD) device is a well-established tool for the treatment of unruptured intracranial aneurysms. Time-of-flight (TOF) MR angiography (MRA) is widely used for postoperative assessment after the treatment with FD; however, it cannot fully visualize intra-aneurysmal and intrastent flow signals due to the magnetic susceptibility from the FD. Recently, the utility of MRA with ultra-short TE (UTE) sequence and arterial spin labeling technique in assessing the therapeutic efficacy of intracranial aneurysms treated with metallic devices has been reported, but long image acquisition time is one of the drawbacks of this method. Herein, we introduce a novel UTE MRA using the subtraction method that enables the reduction in susceptibility artifacts with a short image acquisition time.

Keywords: *flow-diverter, intracranial aneurysm, magnetic resonance angiography, ultra-short echo time*

Introduction

A flow-diverter (FD) device has recently been developed as an endovascular stent for the treatment of intracranial aneurysms. It has been applied to large- and wide-neck aneurysms, which were once difficult to treat.[1–4] Since the thrombosis of aneurysms progresses slowly after stent placement, there is a risk of developing an ischemic attack due to in-stent stenosis, periodic monitoring of intra-aneurysmal flow, and stent patency after stent placement is required. In general, a noninvasive time-of-flight (TOF) MR angiography (MRA) is used for evaluation after stent placement; however, it cannot fully visualize intra-aneurysmal and intrastent flow signals due to the magnetic susceptibility of the metallic device. Recent clinical studies have demonstrated the usefulness of noncontrast-enhanced MRA with ultra-short TE (UTE) sequence and arterial spin labeling (ASL) in assessing the therapeutic efficacy of intracranial aneurysms treated with metallic devices, including coils and stents.[5–8] This technique reduces the artifacts that are typically observed after coil or stent placement; however, this has several drawbacks, including the requirement of a long image acquisition time (approximately 7–12 min) and difficulty in evaluating structures other than blood flows.[5–8]

In this report, we introduce a novel UTE MRA technique using the subtraction method (sub-UTE MRA), which enables the reduction in susceptibility artifacts and image acquisition time to assess intracranial aneurysms treated with the FD.

Materials and Methods

Patient and aneurysm characteristics

This retrospective case series was approved by the institutional review board. The need for informed consent for this study was waived due to the retrospective study design. Between May 2020 and October 2020, six large intracranial internal artery aneurysms in six patients undergoing endovascular embolization using an FD device (Pipeline Flex Embolization Device; Covidien, Irvine, CA, USA) were enrolled in this study. The patients' characteristics are summarized in Table 1. We evaluated all patients based on sub-

[1] Central Division of Radiology, Jichi Medical University Saitama Medical Center, Saitama, Saitama, Japan
[2]Department of Radiology, National Defense Medical College, Tokorozawa, Saitama, Japan
[3]Department of Radiology, Jichi Medical University Saitama Medical Center, Saitama, Saitama, Japan
[4]Department of Endovascular Surgery, Jichi Medical University Saitama Medical Center, Saitama, Saitama, Japan
[5]Department of Neurosurgery, Jichi Medical University Saitama Medical Center, Saitama, Saitama, Japan
[6]Department of Radiology, National Center Hospital, National Center of Neurology and Psychiatry, Kodaira, Tokyo, Japan
*Corresponding author: Department of Radiology, National Defense Medical College, 3-2, Namiki, Tokorozawa, Saitama 359-8513, Japan. Phone: +81-4-2995-1689, Fax: +81-4-2996-5214, E-mail: hkouhei917@gmail.com

Received: August 2, 2021 | Accepted: October 20, 2021

Table 1 Patients and aneurysm characteristics

Case	Age	Sex	Location of aneurysm	Aneurysm size (W × D × H) (mm)	Flow-diverter (diameter-length) (mm)	Additional coils	Interval between DSA and MRA (days)
1	67	F	Rt. Cavernous segment	11 × 8 × 6.4	4.75–18	No	0
2	54	F	Lt. Paraclinoid segment	11 × 11 × 7.7	4.0–18	Yes	2
3	75	F	Lt. Paraclinoid segment	13 × 8.0 × 4.5	4.0–18	Yes	1
4	55	F	Lt. Paraclinoid segment	20 × 18 × 18	3.5–20	Yes	0
5	69	F	Lt. Paraclinoid segment	15 × 10 × 9	5.0–18, 5.0–20	No	4
6	82	M	Rt. Cavernous segment	25 × 14.5 × 13.5	5.0–25	No	26

D, depth; DSA, digital subtraction angiography; F, female; H, height; Lt, left; M, male; MRA, MR angiography; Rt, right; W, width.

UTE MRA, TOF MRA, and digital subtraction angiography (DSA), which were performed approximately 6 months postoperatively. DSA was performed for endovascular treatment and postoperative evaluation using the biplane system (Azurion 7 B20/15 ORT; Philips, Amsterdam, The Netherlands). The median interval between DSA and MRA was 1.5 days (range, 0–26 days).

MRA scan technique

All MRIs and MRAs were obtained using a 3T MRI scanner (Vantage Titan 3T; Canon Medical Systems, Tochigi, Japan) using a 32ch phased array head coil. We obtained a sub-UTE MRA image by subtraction method without the ASL technique that has been generally employed in the previous study.[5–8] Image acquisition protocol of sub-UTE MRA is shown in Fig. 1. Briefly, a sub-UTE MRA image was obtained by subtracting from the UTE image with the presaturation pulse from that without the presaturation pulse of the same slice. The imaging parameters of TOF MRA and sub-UTE MRA are summarized in Table 2. The number of segments is one of the key factors for acquiring a clear vessel image on the sub-UTE MRA, and therefore, we determined the appropriate number of segments for optimal visualization of the intracranial artery in healthy subjects before adapting to actual patients. This finding was obtained from our own institutional experience (see Discussion). The scan times of TOF MRA and sub-UTE MRA were 5 min 42 s and 3 min 42 s, respectively.

Image assessment

Images of sub-UTE MRA, TOF MRA, and DSA were independently reviewed by two board-certified radiologists with 10 and 8 years of experience in image evaluation for neurovascular diseases. The sub-UTE MRA and TOF MRA data were transferred to an independent workstation (SYNAPSE VINCENT; FUJIFILM, Tokyo, Japan) equipped with multiplanar reconstruction of the source images and processed as maximum intensity projection images in two orthogonal orientations by a radiological technologist. The in-stent flow observed by sub-UTE MRA and TOF MRA was assessed using a 4-point scale: 1, not visible (signal alteration in the stent was not detected or cannot be assessed); 2, poor (blood flow signals in the stent were slightly visible, but not adequate for diagnosis); 3, acceptable (blood flow signals in the stent were roughly visible, diagnosable images); and 4, excellent (the images were almost equal to DSA). The intra-aneurysmal flow was graded on a 3-point scale: residual aneurysm (RA) (inflow signal is detected in the aneurysmal dome), neck remnant (NR) (inflow signal is detected in the aneurysmal neck), and complete occlusion (CO) (no inflow signal is detected in the aneurysm). For ratings on the TOF MRA, we refer to a conventional T1-weighted image (scan parameters: TR/TE, 2600/10.0 ms; FOV, 20 cm; flip angle, 90°; matrix size, 224 × 320; section thickness, 5 mm; parallel imaging factor, 1.8; number of excitations, 1; inversion time, 1100 ms; scan time, 2 min 6 s) that was performed simultaneously with TOF MRA because the thrombosed aneurysm was reported as a region showing a high-intensity signal on both TOF MRA and T1-weighted image.[9] When the same site in the aneurysm showed a high signal in both TOF MRA and T1-weighted image, we interpreted it as no flow signal. The rate of agreement of intra-aneurysmal flow between DSA and sub-UTE MRA and TOF MRA was assessed. The interobserver agreement of each MRA for each rating was also evaluated.

Statistical analysis

Statistical analyses were performed using a commercially available software program (EZR, ver. 1.53; Jichi Medical University, Saitama, Japan), which is a graphical user interface for R (The R Project for Statistical Computing, ver. 4.0.2; The R Foundation, Vienna, Austria). More precisely, a modified version of R commander is designed to add statistical functions frequently used in biostatistics.[10] Each value is expressed as median, interquartile range, and range. Differences between the two groups were assessed using the Mann–Whitney U test. Statistical significance was set at $P < 0.05$. Weighted κ values were used to determine the

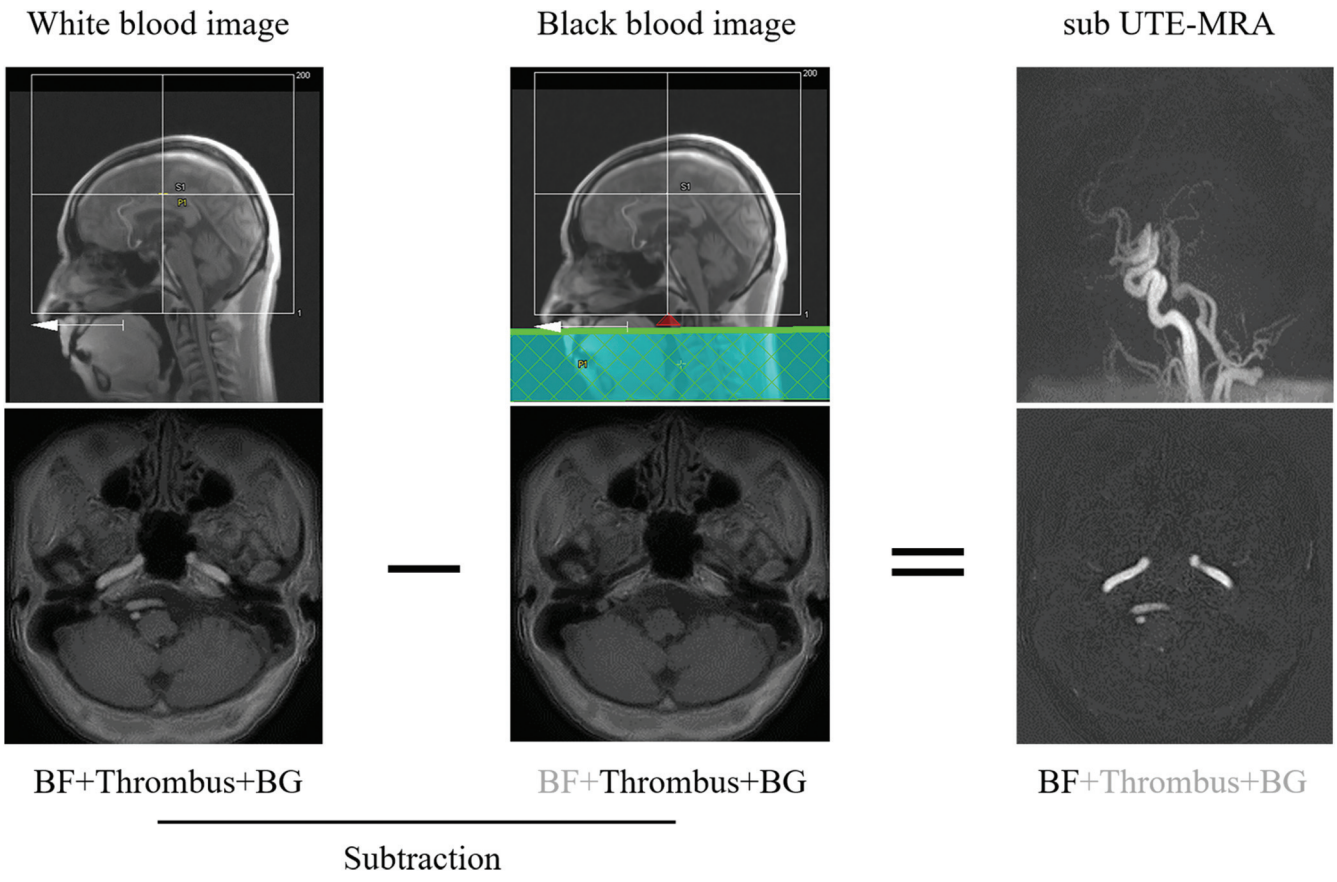

Fig. 1 Post-processing for UTE MRA with the subtraction method (sub-UTE MRA). UTE images without and with a presaturation pulse, which were named as white blood and black blood images, respectively, were acquired in the same slice plane. The square in the upper panel of white blood and black blood image indicates the image acquisition range of the UTE image. The white blood image revealed BF, thrombus, and BG. In this image, the arterial blood flows are visualized as bright signals due to the inflow effect. In the black blood image, the presaturation pulse with 60-mm thickness (green frame in the upper panel) was applied to the cervical vessels located at the 10-mm lower end of the image acquisition range. Since the arterial blood of the tagged region showed a decrease in signal, the signals of arteries were suppressed in the tag-on image. After these images were subtracted, only signals of the arteries were described on the sub-UTE MRA. The upper panel of sub-UTE MRA indicates MIP image. BF, blood flow signals; BG, background; MIP, maximum-intensity projection; MRA, MR angiography; UTE, ultra-short TE.

interobserver agreement. Interobserver agreement was scored as slight ($\kappa < 0.21$), fair ($\kappa = 0.21$ to 0.40), moderate ($\kappa = 0.41$ to 0.60), substantial ($\kappa = 0.61$ to 0.80), and almost perfect ($\kappa = 0.81$ to 1.00).

Results

Results of ratings for in-stent flow and DSA findings are summarized in Table 3. The median score of sub-UTE MRA in assessing in-stent flow was 3 (interquartile range, 3–3; range, 3–3), which was significantly higher than that of TOF MRA, 2 (interquartile range, 1–2; range, 1–2) ($P = 0.002$). The weighted κ value of sub-UTE MRA and TOF MRA regarding stent patency was 1.00, which was almost perfect.

The results of the comparisons of sub-UTE MRA, TOF MRA, and DSA to assess intra-aneurysmal flow are summarized in Table 4. In both readers, the rates of agreement between sub-UTE MRA and DSA and TOF MRA and DSA were 100.0% and 50.0%, respectively. The weighted κ values of sub-UTE MRA and TOF MRA regarding intra-aneurysmal flow was 1.00, which was almost perfect.

A typical image (from case 5) is shown in Fig. 2, in which the in-stent and intra-aneurysmal flow are clearly depicted on sub-UTE MRA compared to TOF MRA. The cases that TOF MRA showed a false positive for assessing intra-aneurysmal flow are shown in Fig. 3. (from case 2) and Fig. 4. (from case 3), respectively. The case that TOF MRA showed a false negative for residual flow in the aneurysmal neck is shown in Fig. 5. (from case 1). In these three cases, sub-UTE MRA provided accurate information regarding intra-aneurysmal flow.

Discussion

In this report, sub-UTE MRA could provide better visualization of the in-stent flow and intra-aneurysmal flow compared

Table 2 MRA scan parameters

	TOF MRA	sub-UTE MRA
TR/TE (ms)	21/3.4	3.7/0.096
Flip angle (°)	15	5
Section thickness (mm)	0.9	1.0
FOV (mm)	210 × 210	230 × 230
Matrix size	256 × 320	320 × 320
Number of excitations	1	1
Parallel imaging factor	2	1
Acquisition voxel size (mm)	0.82 × 0.66	0.72 × 0.72
Number of slices	114	200
Number of coverages	2	1
Number of segments	96	1000
Number of trajectories	N/A	28000
Imaging time	5 min 42 s	3 min 42 s

N/A, not applicable; sub-UTE MRA, subtraction-ultra-short TE MR angiography; TOF MRA, time-of-flight MR angiography.

Table 3 The image score for the in-stent flow observed by TOF MRA sub-UTE MRA

Case	TOF MRA		sub-UTE MRA		DSA
	Reader 1	Reader 2	Reader 1	Reader 2	
1	2	2	3	3	Patent, no stenosis
2	2	2	3	3	Patent, no stenosis
3	2	2	3	3	Patent, no stenosis
4	2	2	3	3	Patent, no stenosis
5	1	1	3	3	Patent, no stenosis
6	2	2	3	3	Patent, no stenosis
	Weighted κ value 1.00		Weighted κ value 1.00		

DSA, digital subtraction angiography; sub-UTE MRA, subtraction-ultra-short TE MR angiography; TOF MRA, time-of-flight MR angiography.

Table 4 Comparison of intra-aneurysmal flow among sub-UTE MRA, TOF MRA, and DSA after the placement of flow-diverter device

Case	TOF MRA		sub-UTE MRA		DSA
	Reader 1	Reader 2	Reader 1	Reader 2	
1	CO	CO	NR	NR	NR
2	RA	RA	NR	NR	NR
3	RA	RA	CO	CO	CO
4	NR	NR	NR	NR	NR
5	NR	NR	NR	NR	NR
6	NR	NR	NR	NR	NR
	Weighted κ value 1.00		Weighted κ value 1.00		

CO, complete occlusion; DSA, digital subtraction angiography; NR, neck remnant; RA, residual aneurysm; sub-UTE MRA, subtraction-ultra-short TE MR angiography; TOF MRA, time-of-flight MR angiography.

with TOF MRA. In addition, this technique provides fewer susceptibility artifacts from stents than the TOF method with a shorter acquisition time. These findings indicate that sub-UTE MRA is useful for assessing intracranial aneurysms treated with an FD device.

TOF MRA is a well-established non-contrast-enhanced MRA technique for assessing intracranial blood flow. However, after endovascular treatment, susceptibility artifacts from metallic devices such as stents and coils have been problematic in depicting aneurysm remnants and stent patency in TOF MRA. In addition, TOF MRA has been reported to show a high-intensity signal in an acute-to-subacute phase of thrombus formation,[9] which may cause false positives in assessing aneurysm remnants. Indeed, in our report, two cases showed false-positive results for detecting aneurysm remnants in TOF MRA.

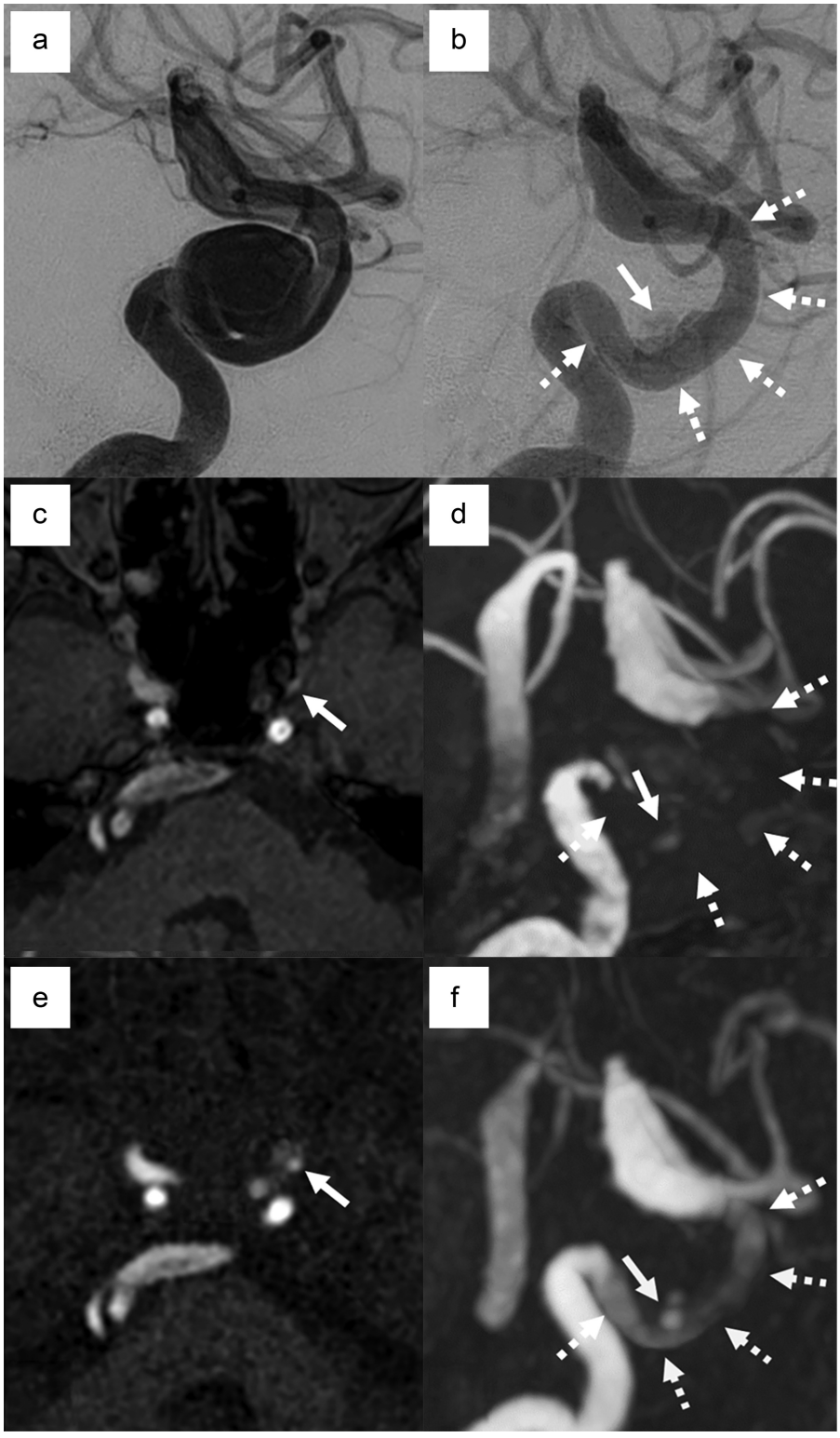

Fig. 2 DSA and MRA findings of case 5. (**a**), DSA of the left internal carotid artery before treatment. (**b**), Six-month follow-up DSA shows residual blood flow in the neck of the aneurysm (arrow) and the patency of the stent (dashed arrows). (**c** and **d**), TOF MRA revealed a punctate high signal in the aneurysm (arrows in **c** and **d**), but the in-stent flow signals were undetectable (dashed arrows in **d**). (**e** and **f**), Sub-UTE MRA clearly visualized the residual blood flow signal in the aneurysm (arrows in **e** and **f**) and in-stent blood flow signal (dashed arrows in **f**). **d** and **f** indicate the MIP image of TOF MRA and sub-UTE MRA, respectively. DSA, digital subtraction angiography; MRA, MR angiography; TOF, time-of-flight; UTE, ultra-short TE.

In that case, it is proposed to evaluate aneurysm remnants by comparing TOF MRA and T1-weighted images, but this may cause false negatives. Furthermore, TOF MRA has shown that signal loss within the artery due to turbulence and/or slow flow often occurs in the cavernous sinus and significant tortuous arteries.[11] In our case series, the blood flow signals in the stent in the cavernous lesions of TOF MRA were relatively weak compared with

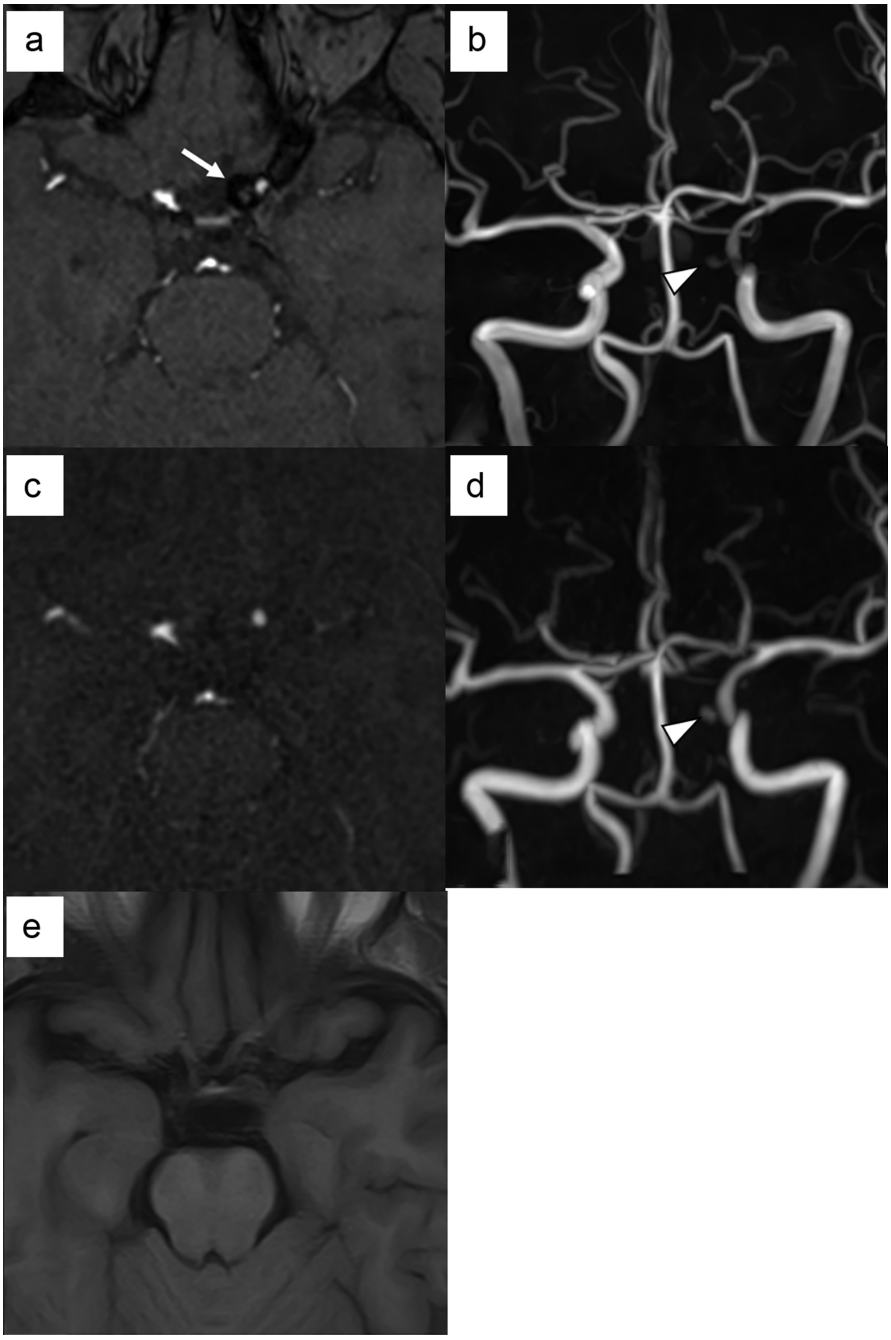

Fig. 3 MRA findings in case 2. (**a** and **b**), TOF MRA. (**c** and **d**), Sub-UTE MRA. (**e**), T1-wighted imaging. **b** and **d** indicate the MIP image of TOF MRA and sub-UTE MRA, respectively. TOF MRA revealed the high signal intensities in the aneurysmal dome (arrow in **a**), although these signal intensities remained unclear in the MIP image (**b**). No obvious high signal intensity was detected on T1-wighted imaging at the sites corresponding to TOF MRA (**e**). Both readers interpreted as residual aneurysm in TOF MRA. Arrow in (**b**) indicates the neck remnant. In the sub-UTE MRA, no flow signals were observed in the aneurysmal dome (**c** and **d**), whereas the high signal intensity in the neck of aneurysm was detected (arrowhead in **d**). Both readers interpreted as neck remnant in sub-UTE MRA. In the DSA, the diagnosis of neck remnant was made. DSA, digital subtraction angiography; MIP, maximum-intensity projection; MRA, MR angiography; TOF, time-of-flight; UTE, ultra-short TE.

those in the other lesions, which could be due to this phenomenon.

UTE MRA is a relatively new MRA technique and has been reported as a useful tool to minimize susceptibility artifacts due to UTE (TE < 0.1 ms). This sequence can reduce the phase dispersion due to metals and other magnetic substances, providing few susceptibility images even after endovascular treatment with metallic devices.[5–8] Furthermore, UTE MRA with the subtraction technique that we proposed in this study and UTE MRA with ASL employed in previous studies did not detect a thrombosis signal in the treated aneurysm because these methods were reconstituted by subtracting the background image from the blood vessel image, which can reduce false positives for assessing the intra-aneurysmal flow that occurs in TOF MRA.

Similar to our report, a previous study demonstrated that UTE MRA with ASL had higher detectability of stent patency and aneurysmal remnant than TOF MRA after the placement of FD device.[5] In that study, the concordance rate

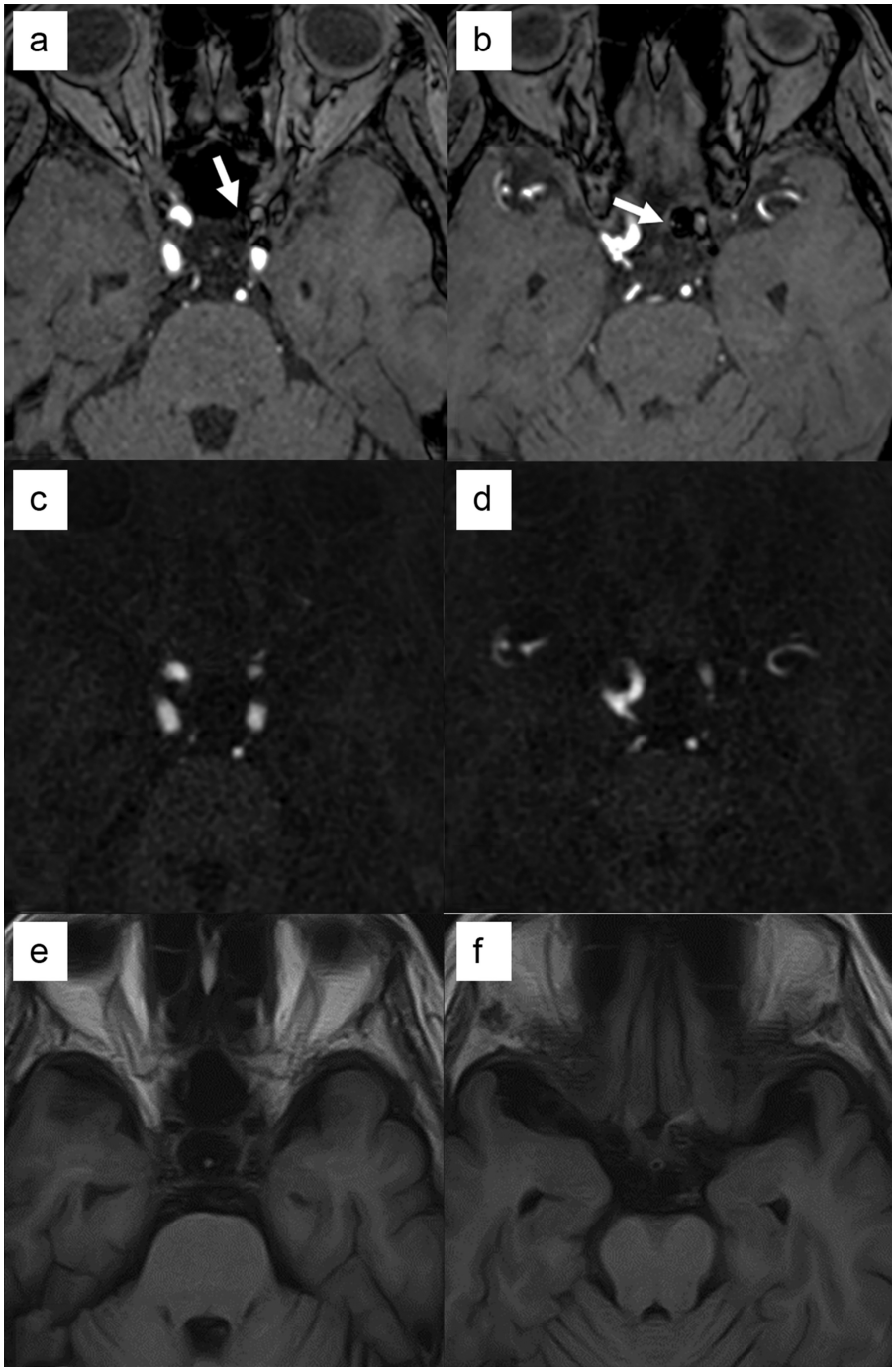

Fig. 4 MRA findings in case 3. (**a** and **b**), TOF MRA. (**c** and **d**), Sub-UTE MRA. (**e** and **f**), T1-wighted imaging. TOF MRA revealed the punctate high signal intensities in both aneurysmal neck and dome (arrows in **a** and **b**, respectively). Since no obvious high signal intensity was detected on T1-wighted imaging at the sites corresponding to TOF MRA (**e** and **f**), both readers interpreted as residual aneurysm in TOF MRA. Sub-UTE MRA showed no flow signals in the aneurysmal dome and neck, and both readers, therefore, interpreted as complete occlusion. In the DSA, the diagnosis of complete occlusion was made. DSA, digital subtraction angiography; MRA, MR angiography; TOF, time-of-flight; UTE, ultra-short TE.

between UTE MRA with ASL and DSA was reported to be as high as 91.0% in the evaluation of intra-aneurysmal blood flow, while that between TOF MRA and DSA was 80.8%. However, the image acquisition time of UTE MRA with ASL in that study was relatively long (approximately 12 min), as it required setting multiple post-labeling delay times after applying the pulse to obtain the desired hemodynamic image. This may reduce the diagnostic ability due to motion artifacts associated with patient intolerance. In addition, a long image acquisition time may disrupt the examination workflow. Sub-UTE MRA can provide UTE MRA by exploiting the inflow effect and subtraction method without the ASL technique. Thus, the image acquisition time can be substantially reduced compared to UTE MRA with ASL without deteriorating image quality, which may improve examination throughput and reduce patient intolerance. In

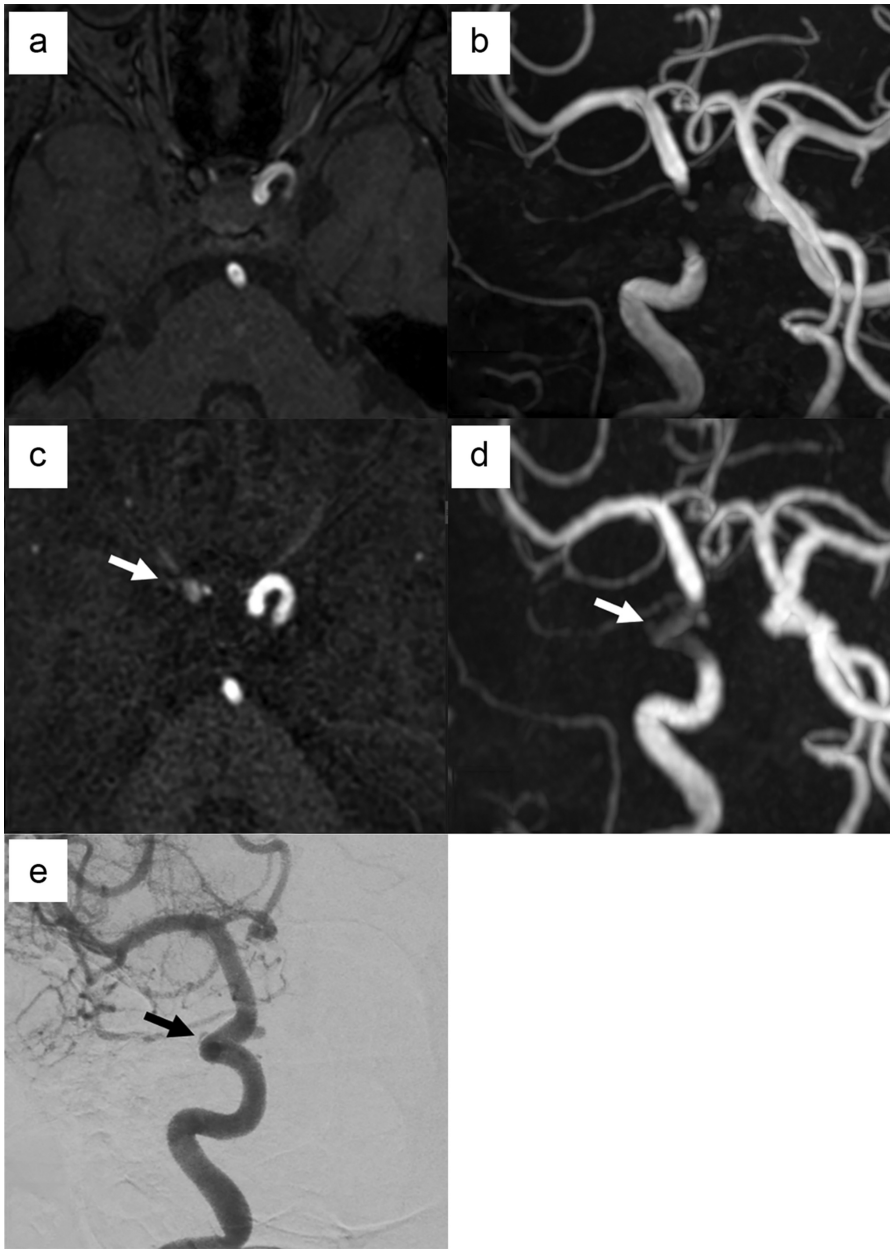

Fig. 5 MRA and DSA findings in case 1. (**a** and **b**), TOF MRA. (**c** and **d**), Sub-UTE MRA. (**e**) DSA. **b** and **d** indicate the MIP image of TOF MRA and sub-UTE MRA, respectively. In TOF MRA, no flow signal was detected in the aneurysm (**a** and **b**). In sub-UTE, the intra-aneurysmal flow signal was observed adjacent to the flow-diverter device (arrows in **c** and **d**), suggesting the neck remnant. On DSA, the neck remnant was observed (arrow in **e**), which was quite similar to the sub-UTE MRA image. DSA, digital subtraction angiography; MIP, maximum-intensity projection; MRA, MR angiography; TOF, time-of-flight; UTE, ultra-short TE.

addition, the short image acquisition time of our method can contribute to the improvement of the examination workflow. Furthermore, our method can depict structures other than blood vessels by referring to the original images, which cannot be visualized by UTE MRA with ASL. This characteristic may help evaluate the anatomical relationship between the therapeutic devices and the target lesion during postoperative evaluation. Although a direct comparison with the UTE MRA with ASL is required, the fact that the detectability of stent patency and aneurysm remnants of sub-UTE MRA was consistent with those of UTE MRA with ASL suggests that sub-UTE MRA is a useful method for the postoperative evaluation of FD device placement, as well as UTE MRA with ASL. We confirmed that the detectability of the stent patency and aneurysmal remnant in sub-UTE MRA and UTE MRA with ASL was equivalent in one case of this case series (data not shown).

The key factor of UTE MRA with the subtraction method is the optimization of the segment number of the k-space trajectory. In the UTE MRA, a tag pulse, including the presaturation pulse and ASL pulse, is applied for each segment, and thus, the segment number increases with the number of tag pulses. Increasing the number of tag pulses, which implies to increasing the number of segments, enhances blood flow signals, resulting in clearer vascular images in the UTE MRA. However, the increase in segment

number leads to a prolonged image acquisition time, and thus, the segment number is generally set to approximately 100 in UTE MRA with ASL. In addition, increasing the number of segments causes an augmentation of background signal in the UTE image with tag pulse (black blood image) due to magnetic transfer effect associated with the application of multiple tag pulses, which leads to the deterioration of the sub-UTE MRA image. Therefore, the optimal number of segments should be determined in consideration of the balance between imaging time and image quality. In the present report, we determined that the appropriate number of segments for sub-UTE MRA would be 1000 by evaluating the images acquired in the same sequence with the number of segments ranging from 100 to 4000 in healthy subjects (Supplementary Fig. 1), which allowed clear visualization of blood flow signals without substantial prolongation of imaging time. The reason that the imaging time was not prolonged despite increasing the number of segments up to 1000 is that our method is a simple subtraction method, which does not require a delay time after applying the tag pulse, such as UTE MRA with ASL.

Despite these advantages, there are some limitations of sub-UTE MRA compared to TOF and UTE MRA with ASL. First, the spatial resolution of our method is relatively lower than that of TOF, although it is almost equivalent to UTE MRA with ASL. Second, our method cannot provide hemodynamic information such as UTE MRA with ASL. However, our method could visualize blood flow in the stent and aneurysm, similar to DSA, and is considered sufficient as an imaging method to determine the therapeutic effect of FD device. The spatial resolution may be improved using deep learning reconstruction and higher magnetic field MRI scanners to achieve higher SNRs. Further validation studies are warranted to clarify the utility of sub-UTE MRA.

Conclusion

Sub-UTE MRA is a useful technique for assessing intracranial aneurysms after the placement of FD device with less acquisition time and artifacts. Our method could be applied to postoperative evaluation after endovascular treatment using other metal devices, including metallic coils and stents.

Conflicts of Interest

The authors declare that they have no conflicts of interest.

Supplementary Information

A Supplementary file below is available online.

Supplementary Fig. 1

The process for determining the optimal number of segments for UTE-MRA. The source image of sub-UTE MRA with the number of segments 100, 500, 1000, 2000, 3000, and 4000. The number in each image indicates the number of segments. Note that the vascular signal increases as the number of segments increases, but the background signal is also augmented in the images with a number of segments more than 1000.

References

1. Kallmes DF, Hanel R, Lopes D, et al. International retrospective study of the pipeline embolization device: a multicenter aneurysm treatment study. AJNR Am J Neuroradiol 2015; 36:108–115.
2. Becske T, Brinjikji W, Potts MB, et al. Long-term clinical and angiographic outcomes following Pipeline embolization device treatment of complex internal carotid artery aneurysms: Five-year results of the Pipeline for uncoilable or failed aneurysms trial. Neurosurgery 2017; 80:40–48.
3. Rangel-Castilla L, Munich SA, Jaleel N, et al. Patency of anterior circulation branch vessels after Pipeline embolization: longer-term results from 82 aneurysm cases. J Neurosurg 2017; 126:1064–1069.
4. Brinjikji W, Murad MH, Lanzino G, et al. Endovascular treatment of intracranial aneurysms with flow diverters: a meta-analysis. Stroke 2013; 44:442–447.
5. Oishi H, Fujii T, Suzuki M, et al. Usefulness of silent MR angiography for intracranial aneurysms treated with a flow-diverter device. AJNR Am J Neuroradiol 2019; 40:808–814.
6. Irie R, Suzuki M, Yamamoto M, et al. Assessing blood flow in an intracranial stent: A feasibility study of MR angiography using a silent scan after stent-assisted coil embolization for anterior circulation aneurysms. AJNR Am J Neuroradiol 2015; 36:967–970.
7. Takano N, Suzuki M, Irie R, et al. Non-contrast-enhanced silent scan MR angiography of intracranial anterior circulation aneurysms treated with a low-profile visualized intraluminal support device. AJNR Am J Neuroradiol 2017; 38:1610–1616.
8. Tanoue S, Uchiyama Y, Hirohata M, et al. Follow-up non-contrast MRA after treatment of intracranial aneurysms using microcoils with prominent metallic artifact: a comparative study of TOF-MRA and Silent MRA. Jpn J Radiol 2020; 38:853–859.
9. Renard D, Le Bars E, Arquizan C, et al. Time-of-flight MR angiography in cerebral venous sinus thrombosis. Acta Neurol Belg 2017; 117:837–840.
10. Kanda Y. Investigation of the freely available easy-to-use software 'EZR' for medical statistics. Bone Marrow Transplant 2013; 48:452–458.
11. Wallace RC, Karis JP, Partovi S, et al. Noninvasive imaging of treated cerebral aneurysms, part I: MR angiographic follow-up of coiled aneurysms. AJNR Am J Neuroradiol 2007; 28:1001–1008.